

Circular arc approximation by quintic polynomial curves

Lian Fang¹

Unigraphics Solutions Inc., 10824 Hope St., Cypress, CA 90630, USA

Received July 1997; revised February 1998

Abstract

This paper presents methods for approximating circular arcs using quintic polynomial curves. Different boundary conditions are considered in the approximation methods, thus resulting approximation curves with G^2 , G^3 , or G^4 continuities at the circular arc's ends. The resulting approximation radial errors are generally very small and converge at the eighth or tenth power of the circular arc's angular span. © 1998 Elsevier Science B.V.

Keywords: Circular arc approximation; Quintic polynomial; Bézier curves; Geometric continuity

1. Introduction

Approximating circular arcs by polynomial curves is a fundamental issue in the practice of computer-aided design. A polynomial representation for circular arcs is not only simpler for the rendering and curve–curve intersection problems, it is of special interest to the aircraft and the automobile industries where surfaces are frequently constructed from curves involving circular arcs using lofting or skinning techniques. In such a surface construction procedure, it is necessary to represent circular arcs in the NURBS form, which often makes the circular arcs become only C^1 and G^2 continuous (but not C^2) due to the presence of interior knots with high multiplicity. This continuity reduction will be inherited onto the constructed surface, thus causing undesired creases. Approximating circular arcs by polynomial curves allows the constructed surfaces to have higher degree of continuity along interior patch boundaries. When the major purpose of approximating circular arcs is to facilitate the downstream processes, the approximating curve is often required to interpolate the given arc's end points and end tangents to ensure that multiple approximating curves can be joined with at least G^1 continuity.

¹ E-mail: fang@ugsolutions.com.

In this paper, a systematic approach for the approximation of circular arcs using quintic polynomials will be presented. The radial approximation error is first analyzed, and different boundary conditions are enforced, thus resulting approximation curves with G^2 , G^3 , or G^4 continuities at the circular arc's ends. Some methods will produce quintic curves that are C^2 joinable. The approximation accuracy and the convergence rate for each method are also evaluated in terms of the radial error and two auxiliary error measurements: the error in curvature and the error in curvature's variation.

The rest of the paper is organized as follows. After a review of the literature in circular arc approximation in Section 2, Section 3 gives some preliminary descriptions about the circular arc, the approximating curve in the Bézier form and the compatibility equations for G^2 , G^3 and G^4 continuities. Section 4 gives the analytic derivation and analysis of the radial approximation error and Section 5 describes several methods for approximating circular arcs using quintic polynomial curves. Section 6 gives the numeric results on the radial error and the auxiliary error measurements.

2. Literature review

Most of the previous work on circular arc approximation is based on cubic polynomial curves. A popular method is to force the parametric mid-point of a cubic curve, matching the arc's end points and end tangents, to coincide with the mid-point of the arc being approximated. To the author's knowledge, the earliest appearance of this method is in (Peters, 1974). It was also discussed in (Gossling, 1976) with a rough numerical error estimate. In (Blinn, 1987), the result of applying this method on a quarter circle is used to improve the performance of circle's rendering since polynomials can be evaluated more quickly using the forward differences technique. In (Dokken, 1990; Goldapp, 1991), this method received more detailed investigations. Not only the extremal value for the radial error and its location are analytically derived, the cubic curve thus created is also proven to be always outside the circular arc. They also prove that the optimal G^1 cubic approximation curve can be obtained by placing the parametric mid-point slightly to the inside of the arc, making the radial error equioscillate three times.

The approximation accuracy can be further improved by allowing the cubic curve not to match the end tangents or even the end points of the arc (Goldapp, 1991). The cubic curve is obtained by solving a nonlinear equation set of two or three variables numerically. Although these methods can achieve an approximation with smaller radial error, their applications are greatly restricted due to the incurred high computation cost and the failure in satisfying the G^1 continuity requirement. In (de Boor, 1987), a method was developed to create a cubic curve interpolating given two points, two tangents and two curvatures, and the solution exists only when certain criteria are met. When applying this method onto circular arc approximation, the resulting cubic curve is G^2 continuous at the curve's ends; however, the approximation accuracy is much lower than using the first method (see Table 4 for a comparison). This is conceivable because the cubic curve, when required to interpolate more boundary conditions, does not have as many degrees of freedom to match the circular arc's shape.

Articles addressing circular arc approximation by quintic polynomial curves are relatively few. In (Bézier, 1986), a quintic Bézier curve, also interpolating the circular arc's end points, end tangents and the mid-point, is given as a good approximation of a semi-circle. There is neither derivation nor explanation about how this quintic curve is obtained; hence, a generalized formula for approximating arcs of arbitrary angular spans is not available. Although approximations of arbitrary arcs can be obtained by subdividing the approximation curve of a semi-circle using the de Casteljau algorithm, the approximation accuracy will not change and the resulting curve will not match the arc's end points and end tangents. Recently, Floater presented a framework for approximating a conic section, in the form of a single rational quadratic Bézier curve, by a Hermite interpolant of odd degree (Floater, 1997). Applying Floater's approach with quintic curves on circular arcs, one can find that the resulting curve has G^3 continuity at the ends and interpolates the arc's mid-point. In Section 5, we will show that this quintic curve is just one of the three quintic curves satisfying the same geometric conditions.

3. Some preliminary

Without loss of generality, we assume that the circular arc's center is located at the origin of the coordinate system and the arc is divided into two sectors symmetrically by the y -axis as shown in Fig. 1. A circular arc of angular span Θ can then be written as

$$\mathbf{A}(u) = (\cos u, \sin u), \quad u_0 = \frac{1}{2}(\pi - \Theta) \leq u \leq \frac{1}{2}(\pi + \Theta) = u_1, \quad 0 < \Theta \leq \pi. \quad (1)$$

Only unit circular arcs are considered here. The approximation of circular arcs of arbitrary radii and orientations can be obtained by radial scaling and rotation. Because the circular arc is symmetric to the y -axis, the approximating curve needs to be symmetric to the y -axis too. From this symmetry, we can immediately infer some properties of the approximating curve, for example, the approximating curve's parametric mid-point should lie on the y -axis and the tangent vector at this point should be parallel to the x -axis.

Given a circular arc described by (1), we want to find a quintic polynomial curve that is at least G^2 continuous at the curve's ends. For convenience, approximation curves that are G^n continuous at the circular arc's end points are called G^n approximations of the

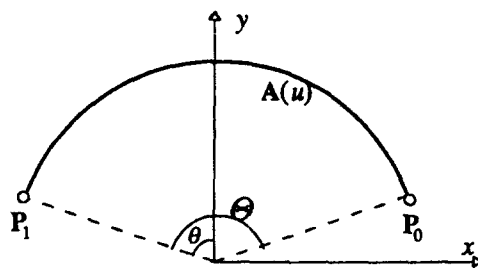


Fig. 1. The circular arc to be approximated.

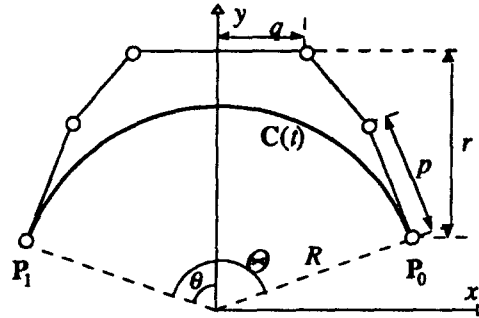


Fig. 2. The approximating quintic curve represented in the Bézier form.

circular arc hereafter. At the beginning, we consider the quintic polynomial curve that is only a G^1 approximation of the arc. Because of the curve's symmetry, this quintic polynomial curve, represented in the Bézier form, can be characterized by three scalars: p , q , and r as shown in Fig. 2 and is written as

$$C(t) = (x(t), y(t)) = \sum_{i=0}^5 B_i \binom{5}{i} (1-t)^{5-i} t^i, \quad \text{for } t \in [0, 1], \tag{2}$$

where

$$\begin{aligned} B_0 &= (\sin \theta, \cos \theta), \quad B_1 = (\sin \theta - p \cos \theta, \cos \theta + p \sin \theta), \quad B_2 = (q, r + \cos \theta), \\ B_3 &= (-q, r + \cos \theta), \quad B_4 = (-\sin \theta + p \cos \theta, \cos \theta + p \sin \theta), \\ B_5 &= (-\sin \theta, \cos \theta) \quad \text{and} \quad \theta = \Theta/2. \end{aligned}$$

It is well known from the differential geometry that if $C(t)$ and $A(u)$ are G^n continuous at a common point $C(\bar{t}) = A(\bar{u})$, their first n derivatives at $t = \bar{t}$ and $u = \bar{u}$ will be related by a connection matrix. The following equation shows such a relationship for G^4 continuity:

$$\begin{bmatrix} C'(\bar{t}) \\ C''(\bar{t}) \\ C'''(\bar{t}) \\ C''''(\bar{t}) \end{bmatrix} = \begin{bmatrix} \alpha_1 & 0 & 0 & 0 \\ \alpha_2 & \alpha_1^2 & 0 & 0 \\ \alpha_3 & 3\alpha_1\alpha_2 & \alpha_1^3 & 0 \\ \alpha_4 & 3\alpha_2^2 + 4\alpha_1\alpha_3 & 6\alpha_1^2\alpha_2 & \alpha_1^4 \end{bmatrix} \begin{bmatrix} A'(\bar{u}) \\ A''(\bar{u}) \\ A'''(\bar{u}) \\ A''''(\bar{u}) \end{bmatrix}. \tag{3}$$

The α_i s in (3) are arbitrary constants. The connection matrix for G^n ($n \leq 3$) continuity is just the submatrix formed by the first n rows and first n columns of the lower triangular matrix in (3). Therefore, for a G^1 approximation curve described by (2), we have $\alpha_1 = 5p$. If $C(t)$ is a G^2 approximation curve, the second derivative of $C(t)$ at $t = 0$ have to satisfy

$$C''(0) = \alpha_1^2 A''(u_0) + \alpha_2 A'(u_0). \tag{4}$$

The equation for $C''(1)$ is similar due to the curve's symmetry, hence, is not shown here. The x and y components of (4) give

$$\begin{cases} 20(q - \sin \theta + 2p \cos \theta) = -\alpha_1^2 \sin \theta - \alpha_2 \cos \theta, & (5a) \\ 20(r - 2p \sin \theta) = -\alpha_1^2 \cos \theta + \alpha_2 \sin \theta. & (5b) \end{cases}$$

Taking (5a) $\times \sin \theta +$ (5b) $\times \cos \theta$, (5a) $\times \cos \theta -$ (5b) $\times \sin \theta$ and using $\alpha_1 = 5p$, we have

$$q \sin \theta - \sin^2 \theta + r \cos \theta + \frac{5}{4}p^2 = 0. \quad (6)$$

and

$$\alpha_2 = 20(r \sin \theta + \sin \theta \cos \theta - q \cos \theta - 2p). \quad (7)$$

Eq. (6) can be called the compatibility equation for G^2 continuity because p , q and r have to satisfy this equation to make $C(t)$ a G^2 approximation curve. Following the same procedure, we can also find the compatibility equations for G^3 and G^4 continuities as

$$2(\sin^2 \theta - 2q \sin \theta - r \cos \theta) + 5p(r \sin \theta + \sin \theta \cos \theta - q \cos \theta) - 10p^2 = 0 \quad (8)$$

and

$$\begin{aligned} & 375p^4 + 1680p^2 + 48(-29 \sin \theta \cos \theta + 40q \cos \theta - 30r \sin \theta)p \\ & + 240 \sin^2 \theta (r + \cos \theta)^2 + 48 \cos \theta (1 - 10q \sin \theta)(r + \cos \theta) \\ & + 48(5q^2 \cos^2 \theta + 5q \sin \theta + \cos^2 \theta - 4) = 0. \end{aligned} \quad (9)$$

A spline approximation of a circular arc can be obtained by splitting it into segments, approximating each segment with a Bézier curve and then joining each approximating Bézier curve together. Enforcing G^1 continuity at the segment's ends allows the approximating Bézier curves to be joined to a C^1 continuous B-spline curve. However, enforcing G^2 continuity at the segment's ends does not necessary guarantee a C^2 B-spline curve, unless all the segments have the same angular spans. When G^2 approximation curves can be joined together, forming a C^2 B-spline curve of the same degree, they are said to be C^2 joinable hereafter.

4. The radial error

The approximation accuracy is usually evaluated by the radial error defined as

$$\varepsilon_r(t) = \sqrt{x^2(t) + y^2(t)} - 1 \quad \text{or} \quad \phi_r(t) = x^2(t) + y^2(t) - 1. \quad (10)$$

Both functions have their zero sets and extremal values at the same locations; however, using $\phi_r(t)$ is preferable since there is no square root term involved. It can be shown that when $\phi_r(t)$ is small, then $\phi_r(t) \approx 2\varepsilon_r(t)$. In this paper, the term "radial error" will be interchangeably used to indicate both $\phi_r(t)$ and $\varepsilon_r(t)$.

The components $x(t)$ and $y(t)$ of the quintic Bézier curve given in (2) are

$$x(t) = (1-t)^5 \sin \theta + 5(\sin \theta - p \cos \theta)t(1-t)^4 + 10qt^2(1-t)^3 - 10qt^3(1-t)^2 + 5(p \cos \theta - \sin \theta)t^4(1-t) - t^5 \sin \theta, \quad (11a)$$

$$y(t) = (1-t)^5 \cos \theta + 5(\cos \theta + p \sin \theta)t(1-t)^4 + 10(r + \cos \theta) \times [t^2(1-t)^3 + t^3(1-t)^2] + 5(p \sin \theta + \cos \theta)t^4(1-t) + t^5 \cos \theta. \quad (11b)$$

Since $x(t)$ and $y(t)$ are quintic polynomials, the radial error $\phi_r(t)$ becomes a polynomial of degree 10, and is given as

$$\phi_r(t) = t^2(1-t)^2[A(1-t)^6 + Bt(1-t)^5 + Ct^2(1-t)^4 + Dt^3(1-t)^3 + Ct^4(1-t)^2 + Bt^5(1-t) + At^6], \quad (12)$$

where

$$A = 25p^2 + 20q \sin \theta + 20(r + \cos \theta) \cos \theta - 20, \quad (13a)$$

$$B = q(80 \sin \theta - 100p \cos \theta) + (r + \cos \theta)(120 \cos \theta + 100p \sin \theta) - 120, \quad (13b)$$

$$C = 100q^2 + 10(\cos 2\theta + p \sin 2\theta) - 100q(\sin \theta - p \cos \theta) + 100(r + \cos \theta)^2 + 100(r + \cos \theta)(\cos \theta + p \sin \theta) - 210, \quad (13c)$$

$$D = 52 \cos 2\theta + 50(-p^2 \cos 2\theta + 2p \sin 2\theta) + 200[(r + \cos \theta)^2 - q^2] - 252. \quad (13d)$$

Carefully examining (13a) and (6), we find that A is a multiple of the left-hand side of (6), which implies that A is zero when $C(t)$ is a G^2 approximation. Furthermore, if we substitute the p^2 term in (8) and (9) by $(4/5)(-q \sin \theta + \sin^2 \theta - r \cos \theta)$ from (6), we find that B and C are also multiples of the left-hand side of (8) and (9) respectively. This means that A and B are both zero when $C(t)$ is a G^3 approximation and A , B and C are all zero when $C(t)$ is a G^4 approximation. These discoveries are not coincidences. Actually, they are the direct results from the simple theorem stated below:

If $C(t)$ is G^n ($0 \leq n \leq 4$) continuous with the circular arc given by (1) at $t = \bar{t}$, the first n derivatives of $\phi_r(t)$ will all vanish at $t = \bar{t}$ and $\phi_r(t)$ can be factorized by $(t - \bar{t})^{n+1}$.

The validity of this theorem for $n = 0$ is quite obvious and needs no further explanations. For $1 \leq n \leq 4$, we can rewrite $\phi_r(t)$ as $\phi_r(t) = C(t) \cdot C(t) - 1$, thus

$$\phi_r^{(n)}(t) = \sum_{i=0}^n \binom{n}{i} \cdot C^{(n-i)}(t),$$

and then substitute (3) into $\phi_r^{(n)}(\bar{t})$ to replace all the derivatives of $C(t)$ by the derivatives of $A(u)$. Finally, using the fact that for a unit circular arc $A(u)$, the inner product of its derivatives are either $-1, 0$ or 1 , we can verify that the first n derivatives of $\phi_r(t)$ are all zero at $t = \bar{t}$. With this theorem, the above discoveries can be deduced easily. For example, if $C(t)$ is a G^2 approximation of the circular arc, $\phi_r(t)$ will assume the form $\phi_r(t) = t^3(1-t)^3\psi(t)$, thus forcing A to be zero.

For now, let's consider the G^2 approximation case, i.e., $A = 0$ and $B \neq 0$, therefore, $\phi_r(t)$ becomes

$$\phi_r(t) = t^3(1-t)^3[B(1-t)^4 + Ct(1-t)^3 + Dt^2(1-t)^2 + Ct^3(1-t) + Bt^4]. \quad (14)$$

By letting $\phi'_r(t) = 0$, we find that $\phi_r(t)$ could have at most five extreme points besides 0 and 1. They are

$$t_1 = \frac{1}{2} - \sqrt{\frac{1}{4} - \mu_1}, \quad t_2 = \frac{1}{2} - \sqrt{\frac{1}{4} - \mu_2}, \quad \frac{1}{2}, \quad 1 - t_1 \quad \text{and} \quad 1 - t_2.$$

where

$$\mu_1 = \frac{1}{2 - \Omega_1}, \quad \mu_2 = \frac{1}{2 - \Omega_2}, \quad \Omega_1 = \frac{(4C - 4B) - \sqrt{\Delta}}{6B},$$

$$\Omega_2 = \frac{(4C - 4B) + \sqrt{\Delta}}{6B}, \quad \text{and} \quad \Delta = (4C - 4B)^2 - 12B(5D - 2C - 10B).$$

Note that to ensure that t_1 and t_2 are real numbers and are within $[0, 1/2]$, Δ must be always nonnegative (for $0 \leq \theta \leq \pi/2$) and μ_1 and μ_2 must be within $[0, 1/4]$.

If $C(t)$ is a G^3 approximation, both A and B are zero, but C is nonzero. The $\phi_r(t)$ becomes

$$\phi_r(t) = t^4(1-t)^4[C(1-t)^2 + Dt(1-t) + Ct^2]. \quad (15)$$

There are at most three interior extreme points located at

$$t_1 = \frac{1}{2} - \sqrt{\frac{1}{4} - \frac{4}{5} \frac{1}{2 - \beta}}, \quad \frac{1}{2}, \quad \text{and} \quad 1 - t_1,$$

where $\beta = D/C$. To ensure that t_1 is real and within $[0, 1/2]$, β must not be greater than $-6/5$.

If $C(t)$ is a G^4 approximation, A , B and C are all zero, and $\phi_r(t)$ becomes

$$\phi_r(t) = Dt^5(1-t)^5 \quad (16)$$

with its maximum value $D/1024$ occurred at $t = 1/2$.

5. Circular arc approximation

In this section, we will present several methods for circular arc approximation. The approximation methods are categorized by the continuities they achieved.

5.1. G^2 approximations

As we can see that when $C(t)$ is a G^1 approximation, its shape is decided by three parameters: p , q and r . If $C(t)$ is a G^2 approximation, p , q and r are governed by the compatibility equation shown in (6), which reduces the number of the shape parameters

to two. Because a quintic Bézier curve can be exactly converted into a quintic Hermite curve, which shape is determined by the position and the first two derivatives at its ends, (α_1, α_2) can also be used as the shape parameters.

Method I

In the first method, we will use (α_1, α_2) as the shape parameters and simply set α_2 to zero. This choice is actually not as arbitrary as it might look. We will leave the explanation of its geometric significance to Section 5.4. The remaining parameter α_1 , or p can be determined by forcing $C(t)$ to interpolate the mid-point of the circular arc at $t = 1/2$. As a result, we have

$$\begin{cases} q = \left(1 - \frac{5}{4}p^2\right) \sin \theta - 2p \cos \theta, & (17a) \end{cases}$$

$$\begin{cases} r = -\frac{5}{4}p^2 \cos \theta + 2p \sin \theta & (17b) \end{cases}$$

from (5a,b) with α_2 set to zero, and

$$r = \frac{8}{5}(1 - \cos \theta) - \frac{1}{2}p \sin \theta \quad (18)$$

from $C(1/2) = (0, 1)$. Substituting (18) into (17b), we obtain a quadratic equation for p as

$$25 \cos \theta p^2 - 50 \sin \theta p + 32(1 - \cos \theta) = 0 \quad (19)$$

and the two solutions (for $0 < \theta < \pi/2$) are

$$p_1 = \frac{\sin \theta - \sqrt{(1 - \cos \theta)(1 - \frac{7}{25} \cos \theta)}}{\cos \theta} \quad \text{and}$$

$$p_2 = \frac{\sin \theta + \sqrt{(1 - \cos \theta)(1 - \frac{7}{25} \cos \theta)}}{\cos \theta}.$$

On the other hand, an upper bound for p can be established by substituting (18) into $\cos \theta + r > 1$, which is derived from the convex hull property of Bézier curves, thus

$$p < \frac{6(1 - \cos \theta)}{5 \sin \theta} = \frac{6}{5} \tan \frac{\theta}{2}. \quad (20)$$

Therefore, we can reject p_2 because it does not satisfy (20). The value of r can be obtained from (17b) or (18) and the value of q from (17a) subsequently. When $\theta = \pi/2$ (a semi-circle), the quadratic term of (19) vanishes and we obtain $(p, q, r) = (0.64, 0.488, 1.28)$.

Because of $C(1/2) = (0, 1)$, we have $\phi_r(1/2) = 0$. From (14), this results in $2B + 2C + D = 0$ and $\phi_r(t)$ is simplified to

$$\phi_r(t) = t^3(1-t)^3(1-2t)^2[Ct(1-t) + B]. \quad (21)$$

The Taylor expansion of B and C at $\theta = 0$ give

$$B = \frac{1}{27}\theta^8 - \frac{1}{162}\theta^{10} + O(\theta^{12}) \quad \text{and} \quad C = \frac{1}{81}\theta^{10} + O(\theta^{12}). \tag{22}$$

which show that when θ is small, B and C are both positive, hence $\phi_r(t)$ is always positive. In fact, the numeric results show that $\phi_r(t)$ is always positive even when $\theta = \pi/2$. This means that the approximating curve is always outside the circular arc.

The first two potential interior extreme points of $\phi_r(t)$ are

$$t_1 = \frac{1}{2} - \sqrt{\frac{1}{4} - \mu_1}, \quad t_2 = \frac{1}{2} - \sqrt{\frac{1}{4} - \mu_2},$$

where $\mu_1 = (1/10)(1 - 4\lambda + \sqrt{(1 - 4\lambda)^2 + 15\lambda})$, $\mu_2 = (1/10)(1 - 4\lambda - \sqrt{(1 - 4\lambda)^2 + 15\lambda})$ and $\lambda = B/C$. The Taylor expansions of μ_1 and μ_2 at $\theta = 0$ give

$$\mu_1 = \frac{3}{16}O(\theta^2) \quad \text{and} \quad \mu_2 = \frac{12}{5}\theta^{-2} + \frac{1}{80} + O(\theta^2),$$

from which we can conclude that the maximum value of $\phi_r(t)$, given by $C\mu_1^3(1 - 4\mu_1)(\mu_1 + \lambda)$, occurs at t_1 (and $1 - t_1$) because μ_2 will become negative when θ is small. The Taylor expansion of $\phi_r(t_1)$ at $\theta = 0$ is

$$\phi_r(t_1) = \frac{1}{16384}\theta^8 + O(\theta^{10}), \tag{23}$$

which shows that the maximum radial error decreases with the eighth power of the circular arc's angular span.

Method II

This method chooses p and r so that $C(t)$ interpolates the position and the curvature of the arc's mid-point at $t = 1/2$. Because $C(t)$ will always match the tangent at the arc's mid-point at $t = 1/2$ due to the curve's symmetry, these two interpolation requirements make $C(t)$ become G^2 continuous at $t = 1/2$. Therefore, from the theorem stated in Section 4, we have $\phi_r(1/2) = 0$ and $\phi_r''(1/2) = 0$.

From $\phi_r''(1/2) = 0$, we have $6B - 6C - 5D = 0$. Substituting (13b,c,d) into this equation and using (18) and (6), we obtain

$$\begin{aligned} p^4 + \frac{4}{5} \sin 2\theta p^3 + \frac{8}{25} (1 - \cos \theta) (2 \cos^3 \theta + 2 \cos^2 \theta - 7 \cos \theta - 15) p^2 \\ + \frac{32}{125} \sin \theta (1 - \cos \theta) (16 + \cos \theta - 7 \cos^2 \theta) p \\ + \frac{16}{625} (1 - \cos \theta)^2 (49 \cos^2 \theta - 46 \cos \theta - 31) = 0 \end{aligned} \tag{24}$$

and the four solutions are

$$\begin{aligned}
p_3 &= -\frac{4}{5}(2 - 2\cos\theta)^{1/2} - \frac{2}{5}\sin\theta[\cos^2\theta + 7 + 4(2 + 2\cos\theta)^{1/2}]^{1/2} \\
&\quad - \frac{2}{5}\sin\theta\cos\theta, \\
p_4 &= -\frac{4}{5}(2 - 2\cos\theta)^{1/2} + \frac{2}{5}\sin\theta[\cos^2\theta + 7 + 4(2 + 2\cos\theta)^{1/2}]^{1/2} \\
&\quad - \frac{2}{5}\sin\theta\cos\theta, \\
p_5 &= \frac{4}{5}(2 - 2\cos\theta)^{1/2} - \frac{2}{5}\sin\theta[\cos^2\theta + 7 - 4(2 + 2\cos\theta)^{1/2}]^{1/2} \\
&\quad - \frac{2}{5}\sin\theta\cos\theta \quad \text{and} \\
p_6 &= \frac{4}{5}(2 - 2\cos\theta)^{1/2} + \frac{2}{5}\sin\theta[\cos^2\theta + 7 - 4(2 + 2\cos\theta)^{1/2}]^{1/2} - \frac{2}{5}\sin\theta\cos\theta.
\end{aligned}$$

We can immediately reject p_3 and p_6 because p_3 is always negative and p_6 does not always satisfy (20).

Because of $\phi_r(1/2) = 0$, we have $2B + 2C + D = 0$, together with $6B - 6C - 5D = 0$ obtained from $\phi_r''(1/2) = 0$, we obtain $B/C = -1/4$ and $B/D = 1/6$, therefore, the radial error becomes

$$\phi_r(t) = Bt^3(1-t)^3(1-2t)^4. \quad (25)$$

The Taylor expansion of B at $\theta = 0$ gives

$$B = -\frac{1}{16}\theta^{10} + O(\theta^{12}), \quad \text{when } p = p_4, \quad \text{and} \quad (26a)$$

$$B = -\frac{1}{32}(123 - 55\sqrt{5})\theta^{10} + O(\theta^{12}), \quad \text{when } p = p_5, \quad (26b)$$

which show that using p_5 can achieve a smaller radial error and the radial error resulted by either p_4 or p_5 is always negative when θ is small. The radial error attains its maximum value $27B/50000$ at $t = 1/2 \mp \sqrt{10}/10$ and from (26a,b) the maximum radial error converges at the tenth power of the arc's angular span.

5.2. G^3 approximations

When $C(t)$ is a G^3 approximation, p , q and r have to satisfy both (6) and (8), from which we can represent q and r as functions of p only as

$$q = \frac{5p(-5\sin\theta p^2 - 6\cos\theta p + 4\sin\theta)}{4(5p + 2\sin\theta\cos\theta)} \quad \text{and} \quad (27a)$$

$$r = \frac{-25\cos\theta p^3 + 20\sin\theta p^2 + 8\sin^3\theta}{4(5p + 2\sin\theta\cos\theta)}. \quad (27b)$$

Obviously the parameter best suited as the shape parameter is p .

Method III

In this method, the shape parameter p is determined by letting $C(1/2) = (0, 1)$. From (18) and (27b), we obtain a cubic equation for p as

$$125 \cos \theta p^3 - 150 \sin \theta p^2 + 20(\cos^3 \theta - 9 \cos \theta + 8)p - 8 \sin \theta(3 \cos^2 \theta - 8 \cos \theta + 5) = 0 \quad (28)$$

and the three solutions are

$$p_7 = \frac{2}{5} \sin \theta,$$

$$p_8 = \frac{\sin \theta(3 - \cos \theta) - \sqrt{(1 - \cos \theta)^3(9 + \cos \theta)}}{5 \cos \theta}, \quad \text{and}$$

$$p_9 = \frac{\sin \theta(3 - \cos \theta) + \sqrt{(1 - \cos \theta)^3(9 + \cos \theta)}}{5 \cos \theta}.$$

Again, p_9 is rejected since it is greater than the upper bound of p in (20). When $\theta = \pi/2$ (a semi-circle), the cubic term of (28) vanishes and we obtain two sets of (p, q, r) : $(2/5, 4/5, 7/5)$ by using p_7 and $(2/3, 4/9, 19/15)$ by using p_8 . The approximation curve obtained using $p = p_7$ is actually the same as the degree 5 Hermite interpolant described in (Floater, 1997) when the conic section is a circular arc. As mentioned previously, there are two more quintic curves that satisfy the same geometric conditions.

Because $C(t)$ is a G^3 approximation curve and $C(1/2) = (0, 1)$, we have $B = 0$ and $2B + 2C + D = 0$, thus $2C + D = 0$. The radial error in (15) is simplified to

$$\phi_r(t) = Ct^4(1-t)^4(1-2t)^2 \quad (29)$$

with maximum value $C/3125$ occurred at $t = 1/2 \mp \sqrt{5}/10$. Substituting (27a,b) into (13c) and using $p = (2/5) \sin \theta$, the constant C in (29) turns out to be in a concise form as

$$C = \frac{16(1 - \cos \theta)^5}{1 + \cos \theta}. \quad (30)$$

Eqs. (29) and (30) clearly show that the radial error, resulted by p_7 , is always positive. The Taylor expansion of C at $\theta = 0$ gives

$$C = \frac{1}{4}\theta^{10} + O(\theta^{12}), \quad \text{when } p = p_7, \quad \text{and} \quad (31a)$$

$$C = \frac{1}{8}(123 - 55\sqrt{5})\theta^{10} + O(\theta^{12}), \quad \text{when } p = p_8. \quad (31b)$$

which show that using p_8 can achieve a much smaller radial error and the maximum radial error resulted by either p_7 or p_8 has a convergence rate of 10.

Method IV

This method determines p by letting $\alpha_2 = 0$. Substituting (17a,b), obtained from setting $\alpha_2 = 0$, to (8), the compatibility equation for G^3 continuity, we obtain

$$5(2 - \cos^2 \theta)p^2 + 4 \sin 2\theta p + 2(\cos 2\theta - 1) = 0 \quad (32)$$

and the two solutions are

$$p_{10} = \frac{-2 \sin 2\theta - 2 \sin \theta \sqrt{10 - \cos^2 \theta}}{5(2 - \cos^2 \theta)} \quad \text{and}$$

$$p_{11} = \frac{-2 \sin 2\theta + 2 \sin \theta \sqrt{10 - \cos^2 \theta}}{5(2 - \cos^2 \theta)}.$$

Obviously, p_{10} should be rejected because it is always negative.

Performing the Taylor expansions of C and D at $\theta = 0$ using p_{11} gives

$$C = -\frac{4}{27}\theta^8 + \frac{1}{81}\theta^{10} + O(\theta^{12}) \quad \text{and} \quad D = -\frac{8}{27}\theta^8 - \frac{2}{81}\theta^{10} + O(\theta^{12}), \quad (33)$$

which show that when θ is small, C and D are both negative, hence the radial error, described by (15), is always negative. The numeric results also show that $\phi_r(t)$ is always negative even when $\theta = \pi/2$. This means that the approximating curve is always inside the circular arc. From (33), we can also conclude that the radial error has only one interior extreme point located at $t = 1/2$ since β approaches 2 when θ approaches zero. The Taylor expansions of $\phi_r(1/2)$ at $\theta = 0$ gives

$$\phi_r(1/2) = -\frac{16}{27}\theta^8 + O(\theta^{12}), \quad (34)$$

which shows that the maximum radial error decays at a rate of 8.

5.3. G^4 approximations: Method V

When $C(t)$ is a G^4 approximation, p , q and r have to satisfy (6), (8) and (9). Substituting (27a, b), obtained from (6) and (8), into (9), we obtain a polynomial of degree six for p as

$$\begin{aligned} & \frac{3125}{4}p^6 - \frac{625}{2} \sin 2\theta p^5 + 125(4 \cos^4 \theta - 19 \cos^2 \theta + 3)p^4 \\ & + 100 \sin 2\theta(9 - 5 \cos^2 \theta)p^3 + 20 \sin^2 \theta(49 \cos^2 \theta - 25)p^2 \\ & + 16 \sin^3 \theta \cos \theta(\cos^2 \theta - 25)p - 16 \sin^4 \theta(\cos^2 \theta - 5) = 0. \end{aligned} \quad (35)$$

The solution can be found within just a few iterations using the Newton–Raphson method with p_7 or p_8 as the initial guess. The value of q and r can be found from (26a,b) subsequently. Note that using p_7 and p_8 as initial guess will result in different solutions for (35) and the numeric results show that the solution obtained using p_8 will achieve better approximation accuracy. The radial error function is described by (16) with maximum value occurred at $t = 1/2$. Because the solution of (35) is numerically computed, the radial error's convergence rate cannot be analytically determined; hence, it will be numerically estimated as shown in Section 6.

5.4. Some notes

There are some issues related to the approximation methods described above that are worth some more explanations. The first one is about setting α_2 to zero in method I and IV. Besides being the simplest choice that actually results in simple quadratic equations as shown previously, using $\alpha_2 = 0$ also makes the first two derivatives of $C(t)$ at its ends become orthogonal, a property of a true circular arc. It is a reasonable approach to mimic the property of the target curve we want to approximate. Furthermore, using $\alpha_2 = 0$ allows the resulting quintic curves to become C^2 joinable. This is because the reparametrization involved in the joining process is affine parameter transformation only. When constructing surfaces from curves involving circular arcs of large angular spans, we can approximate the circular arc by a single C^2 quintic B-spline curve with as many segments as the accuracy needs, thus eliminating the creases on the surface that will otherwise be generated.

The second issue is about the mid-point-interpolating scheme adopted by method I, II and III, which always produce one-sided approximation curves with zero radial error at $t = 1/2$. This immediately suggests that it is possible to make the radial error become equioscillating while still satisfying the same boundary conditions. Although this approach will reduce the maximum radial error and produce a more uniform error distribution, experiences show that the typical radial error reduction does not exceed 30% and is always in company with the increase of the curvature error and the computation cost as well. Therefore, this approach is not recommended unless uniform error distribution is essential to the application. In this paper, this approach is only applied on method I to show how the radial error and other error measurements would differ from its mid-point-interpolating counterpart. The numeric results are shown in Table 1 to 3 and Fig. 3 under the name method I-a.

It is obvious that the above-described methods still have not produced the optimal solution within the class of G^2 quintic approximation curves. Approximation accuracy can be further reduced by letting all the five interior extreme points (ref. Section 4) have the same magnitude or even loosening the G^2 continuity requirement. However, doing so will rely on solving a nonlinear equation set of two or more variables to obtain the approximation curve, therefore, they are not discussed in details here.

6. Approximation assessment

Circular arc approximation methods can be assessed by the yielding approximation accuracy, its convergence rate and the computation cost. To evaluate the approximation accuracy, some sorts of error measurements need to be established first. Although radial error is the most commonly used error measurement, using radial error alone is often insufficient. Therefore, two more auxiliary error measurements are used to help evaluating the approximation accuracy:

- $\varepsilon_k(t) = \|\kappa(t)\| - 1$, measuring the error in curvature, and
- $\varepsilon_v(t) = d\|\kappa(t)\|/ds$, measuring the error in curvature's variation with respect to arc length, which should be zero everywhere for a true arc.

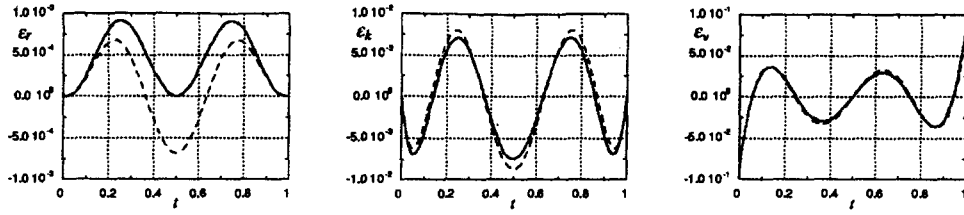


Fig. 3. Distributions of the ε_r , ε_k and ε_v for method I (solid line) and method I-a (dashed line).

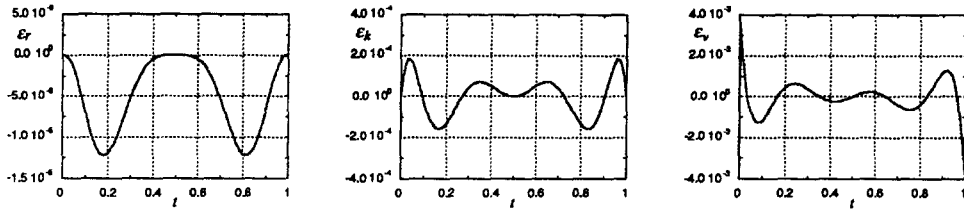


Fig. 4. Distributions of the ε_r , ε_k and ε_v for method II using p_5 .

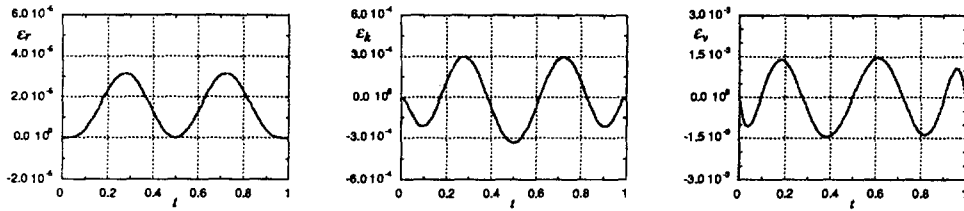


Fig. 5. Distributions of the ε_r , ε_k and ε_v for method III using p_8 .

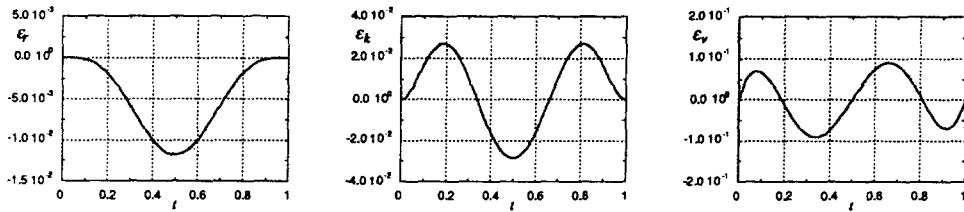


Fig. 6. Distributions of the ε_r , ε_k and ε_v for method IV.

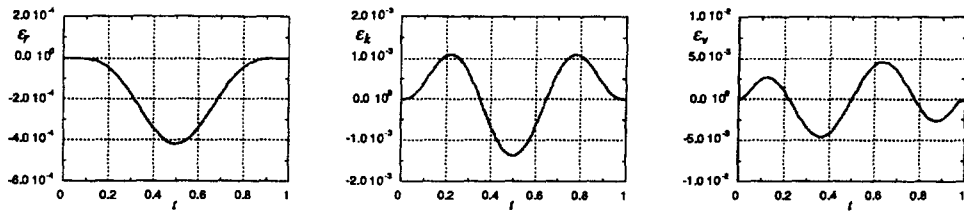


Fig. 7. Distributions of the ε_r , ε_k and ε_v for method V using p_8 as the initial guess.

Table 1
The $|\varepsilon_r|_{\max}$ for circular arcs of angular span Θ (in degree)

Θ	180	150	120
I	9.1089e-04	2.2455e-04 (7.68)	3.9708e-05 (7.76)
I-a	6.7588e-04	1.6556e-04 (7.72)	2.9126e-05 (7.75)
II- p_5	1.2229e-05	1.9889e-06 (9.96)	2.1490e-07 (9.97)
III- p_7	2.5567e-03	4.5478e-04 (9.58)	5.3319e-05 (9.61)
III- p_8	3.1604e-05	5.0098e-06 (10.1)	5.2981e-07 (10.07)
IV	1.1788e-02	2.6205e-03 (8.25)	4.2759e-04 (8.12)
V	4.1895e-02	6.4863e-05 (10.23)	6.7212e-06 (10.16)
Θ	90	60	30
I	4.1550e-06 (7.85)	1.6764e-07 (7.93)	6.6867e-10 (7.98)
I-a	3.0354e-06 (7.86)	1.2212e-07 (7.92)	4.8629e-10 (7.97)
II- p_5	1.2166e-08 (9.98)	2.1180e-10 (9.99)	2.0739e-13 (10.0)
III- p_7	3.2324e-06 (9.74)	5.9215e-08 (9.86)	5.9813e-11 (9.95)
III- p_8	2.9486e-08 (10.0)	5.0707e-10 (10.0)	4.9272e-13 (10.0)
IV	4.2196e-05 (8.05)	1.6370e-06 (8.01)	6.3858e-09 (8.0)
V	3.6795e-07 (10.10)	6.2514e-09 (10.05)	6.0291e-12 (10.02)

Figs. 3 to 7 show the distribution of $\varepsilon_r(t)$, $\varepsilon_k(t)$ and $\varepsilon_v(t)$ resulted by the various methods described in Section 5 using a semi-circle as example. For method II, III and V in which multiple feasible solutions exist, we only display the result for the one that achieves smaller radial error because the error distributions for the other solution are similar. Because all methods will produce approximation curves with at least G^2 continuity, $\varepsilon_r(t)$ and $\varepsilon_k(t)$ are always zero at $t = 0$ and $t = 1$. For methods that produce G^3 approximating curves, their $\varepsilon_v(t)$ graphs (see Figs. 5 and 6) are zero at $t = 0$ and $t = 1$. Error distributions in Figs. 6 and 7 are very much alike; however, the graphs in Fig. 7 are smoother at the boundaries. The maximum values of these three error measurements for different values of Θ are listed in Tables 1, 2 and 3 respectively.

We had proven that all the approximation methods, except method V, will yield an approximation with either order 8 or 10 of convergence rate for the radial error; however, trying to perform the similar analytic analysis for $\varepsilon_k(t)$ and $\varepsilon_v(t)$ is far more difficult. Therefore, the convergence rate of the radial errors for method V and that of $\varepsilon_k(t)$ and $\varepsilon_v(t)$ are computed numerically by

$$m = \log_2 \left(\frac{|\varepsilon(\theta_2)|_{\max}}{|\varepsilon(\theta_1)|_{\max}} \right) / \log_2 \left(\frac{\theta_2}{\theta_1} \right). \tag{36}$$

Table 2
The $|\varepsilon_k|_{\max}$ for circular arcs of angular span Θ (in degree)

Θ	180	150	120
I	7.4544e-03	2.6106e-03 (5.76)	7.4076e-04 (5.65)
I-a	8.6761e-03	3.0701e-03 (5.70)	8.4594e-04 (5.78)
II- p_5	1.8315e-04	4.3958e-05 (7.83)	7.5742e-06 (7.88)
III- p_7	2.1118e-02	5.5918e-03 (7.29)	1.0869e-03 (7.34)
III- p_8	3.3058e-04	7.4256e-05 (8.19)	1.2103e-05 (8.13)
IV	2.8548e-02	1.0098e-02 (5.70)	2.7708e-03 (5.80)
V	1.3734e-03	3.2865e-04 (7.84)	5.6148e-05 (7.92)
Θ	90	60	30
I	1.4066e-04 (5.78)	1.2956e-05 (5.90)	2.0853e-07 (5.97)
I-a	1.5712e-04 (5.85)	1.4258e-05 (5.92)	2.2752e-07 (5.97)
II- p_5	7.7480e-07 (7.93)	3.0710e-08 (7.96)	1.2118e-10 (7.99)
III- p_7	1.2287e-04 (7.58)	5.2460e-06 (7.78)	2.1659e-08 (7.92)
III- p_8	1.1843e-06 (8.08)	4.5856e-08 (8.02)	1.7939e-10 (8.00)
IV	5.1268e-04 (5.86)	4.6418e-05 (5.92)	7.4006e-07 (5.97)
V	5.6848e-06 (7.96)	2.2328e-07 (7.98)	8.7510e-10 (8.00)

Listed in the parentheses of Tables 1, 2 and 3, the convergence rate for any particular angular span is computed against the immediate neighbor on its left. For radial errors, the numeric results show that the convergence rate for method V is also 10 and the numerically computed convergence rates for the other methods also agree with the analytic results shown in Section 5. It is also noteworthy that the methods (method I, I-a and IV) producing quintic curves that are C^2 joinable have convergence rates of 8 while the other methods have convergence rates of 10. For the errors in curvature and curvature's variation, the convergence rates are two and three orders less than that for radial errors respectively.

Table 4 is a summary as well as a comparison for some published methods and the proposed methods. The approximating curve's degree, the achieved continuity at the curve's boundaries, the maximum radial error for a unit semi-circle, and the radial error's convergence rate are listed for each method. This table clearly shows that using quintic polynomial to approximate circular arcs can achieve higher order continuity, improved approximation accuracy and higher convergence rate at the same time. Note that although method III- p_7 has a larger radial error than that of method I for the semi-circle case, its accuracy improves faster than method I does as the arc's angular span decreases. In fact, as shown in Table 1, method III- p_7 will produce smaller radial error when the angular span is 90 degree and smaller. Among the meth-

Table 3
The $|\varepsilon_r|_{\max}$ for circular arcs of angular span Θ (in degree)

Θ	180	150	120
I	8.7891e-02	4.0094e-02 (4.31)	1.4567e-02 (4.54)
I-a	8.2994e-02	3.7584e-02 (4.34)	1.3577e-02 (4.56)
II- p_5	3.6501e-03	1.0853e-03 (6.65)	2.3978e-04 (6.77)
III- p_7	1.9271e-01	4.8726e-02 (7.54)	9.4334e-03 (7.36)
III- p_8	1.4461e-03	3.9327e-04 (7.14)	8.0721e-05 (7.10)
IV	9.0229e-02	3.5192e-02 (5.16)	1.1397e-02 (5.05)
V	4.5520e-03	1.2327e-03 (7.17)	2.5181e-04 (7.12)
Θ	90	60	30
I	3.7450e-03 (4.72)	5.2217e-04 (4.89)	1.6887e-05 (4.97)
I-a	3.4757e-03 (4.74)	4.8322e-04 (4.87)	1.5601e-05 (4.95)
II- p_5	3.3335e-05 (6.86)	2.0086e-06 (6.94)	1.5969e-08 (6.98)
III- p_7	1.2025e-03 (7.16)	7.4278e-05 (6.87)	5.9844e-07 (6.96)
III- p_8	1.0751e-05 (7.01)	6.2906e-07 (7.00)	4.9145e-09 (7.00)
IV	2.7022e-03 (5.00)	3.5746e-04 (4.99)	1.1228e-05 (4.99)
V	3.2899e-05 (7.07)	1.8951e-06 (7.04)	1.4661e-08 (7.01)

ods presented in this paper, method I and III are the most-recommended ones because they yield accurate approximations with appropriate continuities and the approximation curve can be easily computed by those simple formulas described in Sections 5.1 and 5.2.

7. Conclusion

A collection of circular arc approximation methods using quintic polynomial curves has been presented. The approximation accuracy and the convergence rate have also been analyzed. Although the approximations are not optimal, the resulted high accuracy, high convergence rate, and the simplicity in the computation method will certainly make them attractive for practical applications. It should also be noted that all the presented methods are developed based on the “error-in-radius” criterion. However, approximation methods based on other criteria such as maintaining the arc’s convexity or uniform parametrization or minimizing the error in the arc’s sector area or arc length might also be needed for special applications, and should be worth more investigations in the future.

Table 4
A summary of different circular arc approximation methods

Method	degree	G^n	$ \varepsilon_r _{\max}$	$O(\theta^m)$	Note
deBoor et al.	3	G^2	1.3397e-01	6	
Peters, Gossling	3	G^1	1.8350e-02	6	also interpolates the arc's mid-point
Dokken et al., Goldapp	3	G^1	1.3325e-02	6	$\phi_r(t)$ equioscillates three times
Bézier	5	G^1	2.3469e-05	N/A	also interpolates the arc's mid-point. $(p, q, r) = (0.6714, 0.4375, 1.2643)$
Fang, method I	5	C^2	9.1089e-04	8	also interpolates the arc's mid-point $(p, q, r) = (0.64, 0.488, 1.28)$
Fang, method I-a	5	C^2	6.7588e-04	8	$\varepsilon_r(t)$ equioscillates three times $(p, q, r) = (0.639568, 0.488692, 1.279135)$
Fang, method II- p_5	5	G^2	1.2229e-05	10	also interpolates position and curvature at the arc's mid-point $(p, q, r) = (0.667794, 0.442564, 1.266103)$
Floater Fang, method III- p_7	5	G^3	2.5567e-03	10	also interpolates the arc's mid-point $(p, q, r) = (2/5, 4/5, 7/5)$
Fang, method III- p_8	5	G^3	3.1604e-05	10	also interpolates the arc's mid-point $(p, q, r) = (2/3, 4/9, 19/15)$
Fang, method IV	5	C^2 & G^3	1.1788e-02	8	$(p, q, r) = (0.632456, 0.5, 1.264911)$
Fang, method V	5	G^4	4.1895e-04	10	$(p, q, r) = (0.665547, 0.446310, 1.266557)$

* The maximum radial error and the values for p , q and r are computed based on a unit semi-circle.

Acknowledgement

The author would like to thank George Allen for bringing several listed references to the author's attention. The reviewers' comment and suggestions are also greatly appreciated.

References

- Bézier, P. (1986), *The Mathematical Basis of the UNISURF CAD System*, Butterworth & Co.
- Blinn, J. (1987), How many ways can you draw a circle?. *IEEE Computer Graphics and Applications* 7, 39–44.
- de Boor, C., Hollig, K. and Sabin, M. (1987), High accuracy geometric Hermite interpolation. *Computer Aided Geometric Design* 4, 269–278.
- Dokken T., Dæhlen, M., Lyche, T. and Mørken, K. (1990), Good approximation of circles by curvature-continuous Bézier curves, *Computer Aided Geometric Design* 7, 33–41.
- Floater, M.S. (1997), An $O(h^{2n})$ Hermite approximation for conic sections, *Computer Aided Geometric Design* 14, 135–151.
- Goldapp, M. (1991), Approximation of circular arcs by cubic polynomials, *Computer Aided Geometric Design* 8, 227–238.
- Gossling, T.H. (1976), The 'Duct' system of design for practical objects. in: *Proc. World Congress on the Theory of Machines and Mechanisms*, Milan, 305–316.
- Peters, G.J. (1974), Interactive computer graphics application of the parametric bi-cubic surface to engineering design problems, in: Barnhill, R.E. and Riesenfeld, R.F., eds., *Computer Aided Geometric Design*, Academic Press, New York.